J|A|C|S
ARTICLES
Published on Web 06/19/2002

# Periodic Density Functional Theory Study of Methane Activation over $La_2O_3$: Activity of $O^{2-}$, $O^-$, $O_2^{2-}$, Oxygen Point Defect, and $Sr^{2+}$-Doped Surface Sites

Michael S. Palmer,[†] Matthew Neurock,*[,†] and Michael M. Olken[‡]

*Contribution from the Department of Chemical Engineering, University of Virginia, Charlottesville, Virginia 22903, and Corporate Research—Chemical Sciences, The Dow Chemical Company, Midland, Michigan 48674*

Received September 4, 2001. Revised Manuscript Received February 8, 2002

***Abstract:*** Results of gradient-corrected periodic density functional theory calculations are reported for hydrogen abstraction from methane at $O^{2-}_{(s)}$, $O^{-}_{(s)}$, $O^{2-}_{2(s)}$, point defect, and $Sr^{2+}$-doped surface sites on $La_2O_3(001)$. The results show that the anionic $O^{-}_{(s)}$ species is the most active surface oxygen site. The overall reaction energy to activate methane at an $O^{-}_{(s)}$ site to form a surface hydroxyl group and gas-phase $^{\bullet}CH_3$ radical is 8.2 kcal/mol, with an activation barrier of 10.1 kcal/mol. The binding energy of hydrogen at an $O^{-}_{(s)}$ site is −102 kcal/mol. An oxygen site with similar activity can be generated by doping strontium into the oxide by a direct $Sr^{2+}/La^{3+}$ exchange at the surface. The $O^-$-like nature of the surface site is reflected in a calculated hydrogen binding energy of −109.7 kcal/mol. Calculations indicate that surface peroxide ($O^{2-}_{2(s)}$) sites can be generated by adsorption of $O_2$ at surface oxygen vacancies, as well as by dissociative adsorption of $O_2$ across the closed-shell oxide surface of $La_2O_3(001)$. The overall reaction energy and apparent activation barrier for the latter pathway are calculated to be only 12.1 and 33.0 kcal/mol, respectively. Irrespective of the route to peroxide formation, the $O^{2-}_{2(s)}$ intermediate is characterized by a bent orientation with respect to the surface and an O−O bond length of 1.47 Å; both attributes are consistent with structural features characteristic of classical peroxides. We found surface peroxide sites to be slightly less favorable for H-abstraction from methane than the $O^{-}_{(s)}$ species, with $\Delta E_{rxn}(CH_4) = 39.3$ kcal/mol, $E_{act} = 47.3$ kcal/mol, and $\Delta E_{ads}(H) = -71.5$ kcal/mol. A possible mechanism for oxidative coupling of methane over $La_2O_3(001)$ involving surface peroxides as the active oxygen source is suggested.

## Introduction

Conversion of methane into liquid products is traditionally achieved via steam reforming to produce CO and $H_2$, followed by transformation of these diatomic molecules into oxygenates and higher hydrocarbons. Because the energy input required for steam reformation is exorbitant, alternative routes to methane conversion have been pursued. One approach, which leads to *direct* formation of $C_2$ products, is oxidative coupling. Oxidative coupling of methane (OCM) occurs via a combination of heterogeneous and homogeneous steps in which initial activation of a C−H bond takes place over the surface of a metal oxide to produce $^{\bullet}CH_3$ radicals. Methyl radical recombination then occurs in the gas phase. Despite a general agreement about the overall route for OCM, the reactive surface intermediate responsible for the initial C−H bond activation remains unknown.[1−5]

Studies have shown that rare-earth-metal (REM) sesquioxides are especially effective OCM catalysts.[6,7] These highly basic oxides are capable of achieving >80% selectivity for $C_2$ compounds at over 15% $CH_4$ conversion, with Sr-doped $La_2O_3$ being among the most active materials.[3,5,8] Because of the high activity of $La_2O_3$, a number of experimental investigations have centered around its OCM chemistry. Studies by Lunsford and co-workers have shown that $La_2O_3$, as well as most other REM oxides,[7] produces large amounts of $^{\bullet}CH_3$ radicals under OCM conditions (600 °C and 15 Torr of $O_2$).[9] Several investigators have provided evidence that subsequent coupling between methyl radicals accounts for the observed $C_2$ products.[7,10,11] Lunsford has also shown that molecular oxygen is required to maintain high levels of catalytic OCM activity over $La_2O_3$.[9] Although the exact role of $O_2$ is unclear, isotopic labeling experiments[11−14] and kinetic studies[15] both suggest that $O_2$

* To whom correspondence should be addressed. E-mail: mn4n@virginia.edu.
[†] University of Virginia.
[‡] The Dow Chemical Co.

(1) Lee, J. S.; Oyama, S. T. *Catal. Rev.−Sci. Eng.* **1988**, *30*, 249−280.
(2) Dubois, J.-L.; Cameron, C. J. *Appl. Catal.* **1990**, *67*, 49−71.
(3) Amenomiya, Y.; Birss, V. I.; Goledzinowski, M.; Galuszka, J.; Sanger, A. R. *Catal. Rev.−Sci. Eng.* **1990**, *32*, 163−227.
(4) Voskresenskaya, E.; Roguleva, V.; Anshits, A. G. *Catal. Rev.−Sci. Eng.* **1995**, *37*, 101−143.
(5) Lunsford, J. H. *Angew. Chem., Int. Ed. Engl.* **1995**, *34*, 970−980.
(6) Otsuka, K.; Jinno, K.; Morikawa, A. *J. Catal.* **1986**, *100*, 353−359.
(7) Campbell, K. D.; Zhang, H.; Lunsford, J. H. *J. Phys. Chem.* **1988**, *92*, 750−753.
(8) DeBoy, J. M.; Hicks, R. F. *J. Chem. Soc., Chem. Commun.* **1988**, 982−984.
(9) Lin, C.-H.; Campbell, K. D.; Wang, J.-X.; Lunsford, J. H. *J. Phys. Chem.* **1986**, *90*, 534−537.
(10) Nelson, P. F.; Lukey, C. A.; Cant, N. W. *J. Catal.* **1989**, *120*, 216−230.
(11) Lacombe, S.; Zanthoff, H.; Mirodatos, C. *J. Catal.* **1995**, *155*, 106−116.
(12) Haung, S.-J.; Walters, A. B.; Vannice, M. A. *J. Catal.* **2000**, *192*, 29−47.
(13) Winter, E. R. S. *J. Chem. Soc. A* **1969**, 2889−2902.


**10.1021/ja0121235 CCC: $22.00** 

dissociatively adsorbs over the $La_2O_3$ surface to generate active oxygen species.

The activated forms of surface oxygen most commonly implicated in OCM chemistry are the anion radical $O^-$, the superoxide $O_2^-$, and/or the peroxide $O_2^{2-}$. Kinetic studies of OCM reactions over $Sm_2O_3$ by Otsuka and Jinno indicate that the active oxygen source is likely diatomic,[16] and the developing consensus is that a diatomic oxygen species is indirectly, if not directly, responsible for the activation of methane on many OCM catalysts.

Experimental evidence is mounting in support of peroxides as the active form of oxygen responsible for H-abstraction reactions. Both the groups of Sinev and Otsuka demonstrated that simple peroxides such as $Na_2O_2$, $BaO_2$, and $SrO_2$ are capable of stoichiometric partial oxidation of methane,[17−19] indicating that $O_2^{2-}$ is active for abstracting hydrogen from methane. Kharas and Lunsford were the first to show that peroxide ions exist on a complex metal oxide surface ($BaPbO_3$) and are capable of catalyzing the oxidation of methane to $C_2$ hydrocarbons.[20] In addition, in situ Raman experiments by Lunsford et al. revealed the presence of peroxides on Ba/MgO catalysts at temperatures up to 800 °C.[21] X-ray photoelectron spectroscopy (XPS) studies on the same system showed good correlation between intrinsic catalytic activity and near-surface concentration of peroxide ions.[22] Yamashita et al. also employed XPS and thermal decomposition experiments to detect peroxide ions over $BaO/La_2O_3$.[23] Moreover, Lunsford et al. reported the presence of a Raman band characteristic of $O_2^{2-}$,[24] though subsequent studies failed to reproduce these results.[5] More recently, Au and co-workers have suggested that the interaction between $O_2^{2-}$ ions (observed via in situ Raman) and $CH_4$ may generate carbene radicals, which would account for the highly selective nature of $BaCO_3$/LaOBr catalysts to produce ethylene.[25]

Although Lunsford's group[9,26] and others[27−29] have detected a paramagnetic signal from EPR studies on $La_2O_3$ characteristic of the superoxide ion $O_2^-$, there is some doubt that this species is actually responsible for methane activation. Iwamoto and Lunsford showed that the $O_2^-$ ion is unreactive toward simple alkanes on MgO at temperatures up to 200 °C.[30] Louis and coworkers demonstrated the instability of the superoxide ion on $La_2O_3$ under OCM conditions and suggested that the instability stems from the low partial pressure of oxygen commonly used in the reaction.[27,28] In addition, Otsuka et al. found that $O_2^-$ ions contained in simple peroxides did not activate methane.[17]

Another oxygen species frequently implicated in OCM chemistry on metal oxides is the monatomic anion $O^-$. While there is evidence that $O^-$ sites are responsible for H-abstraction from methane over Li-promoted MgO,[31] the presence of $O^-$ sites has not been detected on $La_2O_3$ or other REM oxides. Despite the lack of experimental evidence, it is not unreasonable to suggest that the highly reactive $O^-$ species could be generated via decomposition of a diatomic oxygen species and account for OCM reactions over REM oxides. In fact, Kazansky and co-workers have noted that each of the oxygen species may exist in equilibrium, depending on the nature of the catalyst (eq 1).[32,33]

$$O_{2(g)} \rightleftharpoons O_{2(ads)} \overset{+e^-}{\rightleftharpoons} O_2^- \overset{+e^-}{\rightleftharpoons} O_2^{2-} \rightleftharpoons 2O^- \overset{+2e^-}{\rightleftharpoons} 2O^{2-} \quad (1)$$

Several theoretical studies on OCM over metal oxides can be found in the literature, most of which are concerned with H-abstraction over MgO and other irreducible oxides.[34−44] Theoretical studies of methane activation have also been reported for the bare oxygen species,[45] and in depth studies have been done on metal oxide ions such as $FeO^+$ due to their potential as enzyme models.[46,47] In comparison, theoretical studies of OCM over $La_2O_3$ or other REM oxides are scarce. To our knowledge, only three such studies have been reported. Capitán and co-workers examined the interaction between $La(OH)_3$ clusters and methane using ab initio Hartree−Fock theory and the effects on OCM imposed by a regular lattice with an embedded cluster method employing point charges.[48] On the basis of the results, they concluded that *heterolytic* splitting of $CH_4$ could occur under OCM conditions but it would take place on basic, lattice oxide sites without requiring the presence of adsorbed oxygen, whereas *homolytic* splitting of $CH_4$ to produce $^\bullet CH_3$ radicals would occur on an adsorbed oxygen species. Au et al. investigated the potential for C−H bond activation by $O^-$, $O_2^{2-}$, $O^{2-}$, and $O_2^{4-}$ by applying second-order Møller−Plesset perturbation theory to small clusters containing seven atoms or less.[45] They found that the overall energy for the reaction between $O^-$ or $O_2^{2-}$ and methane to


(14) Winter, E. R. S. *J. Chem. Soc. A* **1969**, 1832−1835.
(15) Pak, S.; Qiu, P.; Lunsford, J. H. *J. Catal.* **1998**, *79*, 222−230.
(16) Otsuka, K.; Jinno, K. *Inorg. Chim. Acta* **1986**, *121*, 237−241.
(17) Otsuka, K.; Said, A. A.; Jinno, K.; Komatsu, T. *Chem. Lett.* **1987**, 77−80.
(18) Otsuka, K.; Murakami, Y.; Wada, Y.; Said, A. A.; Morikawa, A. *J. Catal.* **1990**, *121*, 122−130.
(19) Sinev, M. Y.; Korchak, V. N.; Krylov, O. V. *Kinet. Katal.* **1986**, *27*, 1274.
(20) Kharas, K. C. C.; Lunsford, J. H. *J. Am. Chem. Soc.* **1989**, *111*, 2336−2337.
(21) Lunsford, J. H.; Yang, X.; Haller, K.; Laane, J. *J. Phys. Chem.* **1993**, *97*, 13810−13813.
(22) Dissanayake, D.; Lunsford, J. H.; Rosynek, M. P. *J. Catal.* **1993**, *143*, 286−298.
(23) Yamashita, H.; Machida, Y.; Tomita, A. *Appl. Catal. A: General* **1991**, *79*, 203−214.
(24) Mestl, G.; Knozinger, H.; Lunsford, J. H. *Ber. Bunsen-Ges. Phys. Chem.* **1993**, *97*, 319−321.
(25) Au, C. T.; He, H.; Lai, S. Y.; Ng, C. F. *J. Catal.* **1996**, *163*, 399−408.
(26) Wang, J.-X.; Lunsford, J. H. *J. Phys. Chem.* **1986**, *90*, 3890−3891.
(27) Louis, C.; Chang, T. L.; Kermarec, M.; Le Van, T.; Tatibouët, J. M.; Che, M. *Catal. Today* **1992**, *13*, 283−289.
(28) Louis, C.; Chang, T. L.; Kermarec, M.; Le Van, T.; Tatibouët, J. M.; Che, M. *Colloids Surf. A: Physiochem. Eng. Aspects* **1993**, *72*, 217−228.
(29) Yang, T.; Feng, L.; Shen, S. *J. Catal.* **1994**, *145*, 384−389.
(30) Iwamoto, M.; Lunsford, J. H. *J. Phys. Chem.* **1980**, *84*, 3079−3084.
(31) Ito, T.; Wang, J.-X.; Lin, C.-H.; Lunsford, J. H. *J. Am. Chem. Soc.* **1985**, *107*, 5062−5068.
(32) Shvets, V. A.; Vrotyntsev, V. M.; Kazansky, V. B. *Kinet. Katal.* **1969**, *10*, 356.
(33) Kazansky, V. B. *Kinet. Katal.* **1977**, *18*, 43−54.
(34) Børve, K. J.; Pettersson, L. G. M. *J. Phys. Chem.* **1991**, *95*, 7401−7405.
(35) Børve, K. J.; Pettersson, L. G. M. *J. Phys. Chem.* **1991**, *95*, 3214−3217.
(36) Børve, K. J. *J. Phys. Chem.* **1991**, *95*, 4626−4631.
(37) Stiakaki, M.-A. D.; Tsipis, A. C.; Xanthopoulos, C. E. *J. Mol. Catal.* **1993**, *82*, 425−442.
(38) Aray, Y.; Rodríguez, J.; Murgich, J.; Ruette, F. *J. Phys. Chem.* **1993**, *97*, 8393−8389.
(39) Johnson, M. A.; Stefanovich, E. V.; Truong, T. N. *J. Phys. Chem. B* **1997**, *101*, 3196−3201.
(40) Mehandru, S. P.; Anderson, A. B. *J. Phys. Chem.* **1987**, *91*, 2930−2934.
(41) Mehandru, S. P.; Anderson, A. B.; Brazdil, A. B. *J. Chem. Soc., Faraday Trans.* **1987**, *83*, 463−475.
(42) Ward, M. D.; Brazdil, J. F.; Mehandru, S. P.; Anderson, A. B. *J. Phys. Chem.* **1987**, *91*, 6515−6521.
(43) Mehandru, S. P.; Anderson, A. B.; Brazdil, J. F. *J. Am. Chem. Soc.* **1988**, *110*, 1715−1719.
(44) Ito, T.; Tashiro, T.; Kawasaki, M.; Watanabe, T.; Toi, K.; Kobayashi, H. *J. Phys. Chem.* **1991**, *95*, 4476−4483.
(45) Au, C.-T.; Zhou, T.-J.; Lai, W.-J.; Ng., C.-F. *Catal. Lett.* **1997**, *49*, 53−58.
(46) Shiota, Y.; Yoshizawa, K. *J. Am. Chem. Soc.* **2000**, *122*, 12317−12326.
(47) Bärsch, S.; Schröder, D.; Schwarz, H. *Chem. Eur. J.* **2000**, *6*, 1789−1796.
(48) Capitán, M. J.; Odriozola, J. A.; Márquez, A.; Sanz, J. F. *J. Catal.* **1995**, *156*, 273−278.

produce an O−H surface species and gas-phase $^{\bullet}CH_3$ radical is exothermic, with a low activation barrier, while the same reaction involving $O^{2-}$ or $O_2^{4-}$ is endothermic with a high activation barrier. Last, Islam and Illet have examined the role of surface structure, structural defects, and oxygen ion migration on the catalytic activity of $La_2O_3$ using atomistic computer simulation techniques formulated within the framework of the Born model.[49−51] Results of their studies indicate that the {001} and {011} surfaces of $La_2O_3$ are the most stable, an $O^{2-}$ Frenkel defect is the predominant intrinsic disorder, oxygen diffusion to and from the surface is facile, and $O_2^{2-}$ peroxide species should be stable on $La_2O_3$ surfaces.

The theoretical studies mentioned above have provided valuable insight into some of the salient features of OCM over rare-earth-metal oxides not easily attainable through experiment. The limitations and approximations of the computational methods employed in the studies reported in the literature, however, have left the theoretical treatment of this system incomplete. In an attempt to fill the void, we report herein the first periodic density functional theory study of methane activation over $La_2O_3$. The periodic approach imparts a number of significant advantages over the methods utilized in the past. For instance, a more realistic representation of the lanthanum oxide surface is employed, size and edge effects commonly associated with cluster models are eliminated, different surface oxygen species can be examined, and surface defect sites and interactions between adsorbates, such as methane and molecular oxygen, and the catalyst surface may be fully explored. In addition, quantitative results for adsorbate binding energies, overall reaction energies, and activation energies are possible.

Following a thorough account of the calculational details, all of the different oxygen sites on $La_2O_3$ that were studied ($O^{2-}$, $O^-$, and $O_2^{2-}$) are examined in full individually. (We have chosen not to investigate the superoxide $O_2^-$ simply because of the wealth of data showing its inactivity for H-abstraction from methane under OCM conditions.) The adsorption energy of hydrogen at each oxygen site is reported, as well as the overall reaction energy for the abstraction of hydrogen from methane to generate surface O−H species and gas-phase $^{\bullet}CH_3$ radicals. In certain instances, the activation barrier for the H-abstraction step is reported. In addition to studying the different oxygen species on the surface of $La_2O_3$, we also explored the effect of $Sr^{2+}$-doping as a way to generate an $O^-$ site, as well as the effect of oxygen point defect sites on methane activation. Oxide ion vacancies introduced into the surface model F-centers (a hole containing two trapped electrons) and changes in the hydrogen adsorption energy at oxygen sites adjacent to F-centers are discussed. In addition, adsorption of molecular oxygen at the surface defect sites is examined. Results indicate that the oxygen species generated is peroxide-like in nature. Characterization and reactivity of the $O_2^{2-}$ surface site are provided. Our calculations suggest that similar peroxide sites can be generated pairwise by dissociative adsorption of molecular oxygen across oxide-covered surfaces; this process is fully examined herein. Finally, general comments are made about the mechanism of OCM over $La_2O_3$ based on our results and others' experimental studies. The discussion includes comments on active site formation, C−H bond activation, and catalyst regeneration.

## Calculational Details

**General Theory.** The calculations reported herein were performed using gradient-corrected periodic density functional theory (DFT) as implemented in the Vienna ab initio simulation (VASP) package.[52−55] In the VASP formalism, a self-consistent solution to the Kohn−Sham equations of local spin density functional theory is obtained by an unconstrained band-by-band minimization of the norm of the residual vector of each eigenstate. Convergence to the electronic ground state is accelerated by optimized charge- and spin-mixing routines. The electron−ion interactions are described by either the projector augmented wave (PAW) method originally proposed by Blöchl[56] and implemented by Kresse[57] and/or the ultrasoft pseudopotential (USP) method of Vanderbilt.[58] Both formalisms allow for a significant reduction in computation time, since the large number of plane waves required to represent the oscillations near the core is approximated. Atomic geometries are optimized by conjugate gradient-based relaxation of the total energy.

For the present study, calculations were performed using a spin-polarized version of VASP.[59] Exchange and correlation corrections were described within the generalized gradient approximation of Perdew and Wang (PW91).[60] Brillouin zone sampling was based on the Monkhörst−Pack scheme.[61] Convergence of the total energy with respect to *k*-point sampling was accelerated for the insulating $La_2O_3$ by the tetrahedron method with quadratic corrections. The La atom was described by the PAW pseudopotential of Kresse.[62] All other atoms were described by the Vanderbilt ultrasoft pseudopotentials generated by Kresse and Hafner.[63] Full relaxation of adsorbate/substrate systems was performed.

In addition to the periodic DFT calculations, a set of cluster/adsorbate calculations was performed using the Amsterdam density functional (ADF) theory program of Baerends and co-worker.[64−66] In the ADF formalism, a series of Kohn−Sham one-electron equations is solved in an iterative manner to determine a self-consistent field electron density. All cluster calculations described here used the exchange correlation potential of Vosko−Wilk−Nusair.[67] Nonlocal gradient corrections for the exchange and correlation energy were computed via methods established by Becke[68] and Perdew,[69] respectively. Relativistic corrections were based on the Pauli formalism. All results were obtained from spin-unrestricted calculations. A Slater-type orbital (STO) basis set of triple-$\zeta$ quality with one polarization function was used for all atoms in the clusters/adsorbates studied (La, O, C, and H). Electrons up to the 4d shell of La and up to the 1s shell of O were frozen. Full geometry optimization, based on a quasi-Newton approach which utilizes the Hessian for computing changes in geometry so as to make the gradients vanish, was performed.

**Surface Construction.** $La_2O_3$ crystallizes in the hexagonal space group $P\bar{3}m1$ ($a = b = 3.939$, $c = 6.136$), with a structure characteristic

(49) Ilett, D. J.; Islam, M. S. *J. Chem. Soc., Faraday Trans.* **1993**, *89*, 3833−3839.
(50) Islam, M. S.; Ilett, D. J. *Catal. Today* **1994**, *21*, 417−422.
(51) Islam, M. S.; Ilett, D. J.; Parker, S. C. *J. Phys. Chem.* **1994**, *98*, 9637−9641.
(52) Kresse, G.; Hafner, J. *Phys. Rev. B* **1993**, *47*, 558−561.
(53) Kresse, G.; Hafner, J. *Phys. Rev. B* **1994**, *49*, 14251−14269.
(54) Kresse, G.; Furthmüller, J. *Phys. Rev. B* **1996**, *54*, 11169−11186.
(55) Kresse, G.; Furthmüller, J. *Comput. Mater. Sci.* **1996**, *6*, 15.
(56) Blöchl, P. E. *Phys. Rev. B* **1994**, *50*, 17953−17979.
(57) Kresse, G.; Joubert, D. *Phys. Rev. B* **1999**, *59*, 1758−1775.
(58) Vanderbilt, D. *Phys. Rev. B* **1990**, *41*, 7892−7895.
(59) Moroni, E. G.; Kresse, G.; Hafner, J.; Furthmüller, J. *Phys. Rev. B* **1997**, *56*, 15629−15646.
(60) Perdew, J. P.; Chevary, J. A.; Vosto, S. H.; Jackson, K. A.; Pederson, M. R.; Singh, D. J.; Frolhais, C. *Phys. Rev. B* **1992**, *46*, 6671−6687.
(61) Monkhorst, H. J.; Pack, J. D. *Phys. Rev. B* **1976**, *13*, 5188−5192.
(62) Kresse, G., personal correspondence.
(63) Kresse, G.; Hafner, J. *J. Phys.: Condens. Matter* **1994**, *6*, 8245−8257.
(64) Baerends, E. J.; Ellis, D. E.; Ros, P. *Chem. Phys.* **1973**, *2*, 41−51.
(65) Baerends, E. J.; Ros, P. *Int. J. Quantum Chem. Symp.* **1978**, *12*, 169−190.
(66) Boerrigter, P. M.; Velde, G.; Baerends, E. J. *Int. J. Quantum Chem.* **1988**, *33*, 87−113.
(67) Vosko, S. H.; Wilk, L.; Nusair, M. *Can. J. Phys.* **1980**, *58*, 1200−1211.
(68) Becke, A. D. *Phys. Rev. A* **1988**, *38*, 3098−3100.
(69) Perdew, J. P. *Phys. Rev. B* **1986**, *33*, 8822−8824.

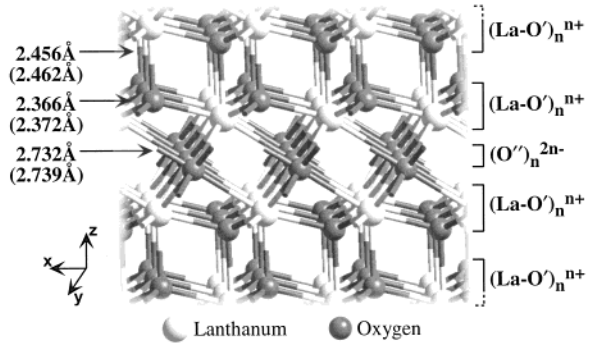


***Figure 1.*** Experimental structure for bulk $La_2O_3$ ($a = b = 3.939$ Å, $c = 6.136$ Å); $(La-O')_n^{n+}$ (O′ represents a four-coordinate oxygen atom) is characterized as a double-hexagonal layer, and $(O'')_n^{2n-}$ (O″ represents a six-coordinate oxygen atom) is an oxygen hexagonal layer. The experimental values for the three unique La−O bond lengths are shown; the bond lengths shown in parentheses are for bulk $La_2O_3$ at the optimized equilibrium lattice constants, $a = b = 3.95$ Å and $c = 6.15$ Å.

of other A-type sesquioxides (Figure 1).[70−72] The calculated equilibrium PW91 lattice constants for bulk $La_2O_3$ are $a = b = 3.95$ Å and $c = 6.15$ Å, which are in good agreement with the experimental values. The unit cell consists of one independent La atom and two independent oxygen atoms. Each La atom is seven-coordinate and possesses a "capped" octahedron geometry with local $C_{3v}$ symmetry. With respect to the *z*-direction indicated in Figure 1, each La atom is bound on one side by six-coordinate oxygen atoms (O″) with local $O_h$ symmetry (each La−O″ bond distance is 2.739 Å) and on the opposite side by four-coordinate oxygen atoms (O′) with local $C_{3v}$ symmetry (three La−O′ bonds are 2.372 Å; one La−O′ bond is 2.462 Å). Coordination between the La and the four-coordinate oxygen atoms forms a dyad of $(LaO')_n^{n+}$ double-hexagonal layers (La−O′−O′−La stacking); the distance between adjacent $(LaO')_n^{n+}$ double-hexagonal layers is 2.462 Å. Each pair of double-hexagonal layers is connected by an $(O'')_n^{2n-}$ layer.

A number of experimental studies[73−76] as well as the theoretical work by Islam and Illet[50,51] indicate that $La_2O_3(001)$ is the most stable surface of lanthanum oxide. Consequently, all calculations described in this report were carried out on supercells constructed from this particular surface. An $La_2O_3(001)$ slab exposing four-coordinate oxygen atoms (O′) on both faces was found to be the most stable. Exposure of either La or O″ atoms resulted in high-energy surfaces. Since Islam and Illet reported similar findings, we did not investigate these particular surface models in any detail. In most calculations, the $La_2O_3(001)$ substrate was modeled by a symmetric, stoichiometric $2 \times 1$ surface cell comprised of 10 atomic layers, four lanthanum and six oxygen. We found that thinner slabs did not consistently model the bulklike properties of the material, and thicker slabs led to insignificant changes in energy. A 12 Å vacuum layer was placed above the surface to avoid any electronic interactions between slabs. A $3 \times 5 \times 1$ Monkhörst−Pack *k*-point grid was used to model the first Brillouin zone. The basis set was restricted to plane waves with a maximum kinetic energy $E_{cut} = 396$ eV. Extensive testing showed that these parameters result in convergence to within 2 meV.

Surface $O^-$ sites were modeled with an asymmetric, nonstoichiometric $2 \times 2$ surface cell comprised of eight atomic layers, three lanthanum and five oxygen (12 Å vacuum layer, $3 \times 3 \times 1$ Monkhörst−Pack *k*-point grid). The larger supercell was necessary to stabilize the bulk of this higher energy surface. Smaller $1 \times 1$ surface cells were also explored, and we found that, in most cases, the smaller cell was capable of accurately modeling adsorbate/oxide interactions; that is, coverage effects had only a small influence on adsorption energies and overall reaction energies. The larger cells were utilized, however, so that multiple active surface sites as well as "isolated" surface defect sites could be investigated.

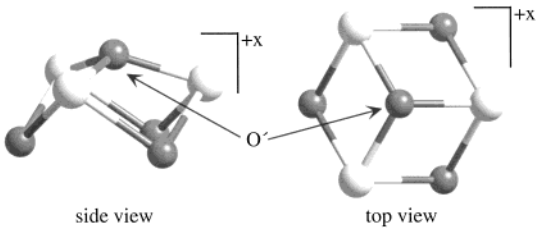


***Figure 2.*** Structure of the seven-atom $[La_3O_4]^{x+}$ cluster used in the ADF calculations.

**Cluster Construction.** Seven atom clusters consisting of three lanthanum atoms and four oxygen atoms were constructed from the {001} surface of $La_2O_3$ (Figure 2). The upper oxygen (O′) and three central lanthanum atoms of the cluster can be viewed as being derived from the $(La-O')_n^{n+}$ layer of $La_2O_3$ and the lower three oxygen atoms derived from an adjacent $(O'')_n^{2n-}$ layer. Appropriate charges were given to the clusters in order to maintain stoichiometry (formal charges of $La^{3+}$ and $O^{2-}$ were assumed); thus, the clusters $[La_3O_4]^+$ and $[La_3O_4]^{2+}$ were used to model surface $O^{2-}$ and $O^-$ sites, respectively. A similar set of clusters were used in the theoretical studies of Au et al.[45]

**Energy Calculations.** Adsorption energies were computed by subtracting the sum of energies of the optimized gas-phase adsorbate and the clean $La_2O_3$ surface from the energy of the optimized adsorbate−surface complex (eq 2). A similar approach was used for

$$\Delta E_{ads} = E_{adsorbate/surface} - (E_{adsorbate} + E_{surface}) \qquad (2)$$

the adsorbate/cluster systems. Overall reaction energies were calculated such that the sum of energies of reactants was subtracted from the sum of energies of products (eq 3). These conventions (eqs 2 and 3) lead to

$$\Delta E_{rxn} = \sum E_{products} - \sum E_{reactants} \qquad (3)$$

negative values for adsorption energies and exothermic reaction energies.

Activation energies for the abstraction of hydrogen from methane over the different oxygen intermediates were estimated by performing a series of single-point calculations at discrete points along the reaction coordinate. Appropriate points were chosen by performing a linear extrapolation between reactant and product states. For the present study, the reactant state was the optimized substrate plus gas-phase molecule, and the product state was the optimized substrate/adsorbate complex. The activation energy for the dissociative adsorption of molecular $O_2$ was determined from a series of single-point calculations along different two-dimensional reaction coordinates. Once an approximate activation barrier for dissociation was identified, the $O_2$ moiety was fixed in space, and the surface layers of the $La_2O_3$ substrate were allowed to relax. The resultant energy was taken to be the activation barrier. (Complete details can be found in a preliminary publication.[77]) Since full relaxation of the ions was not allowed, the activation energies reported herein can be considered an upper bound to the actual barriers.

## Results and Discussion

**Hydrogen Abstraction over Surface $O^{2-}$ Sites.** Oxide ($O^{2-}$) surface sites on $La_2O_3$ were modeled with a symmetric slab containing four lanthanum layers and six oxygen layers. The slab was constructed by cleaving $La_2O_3(001)$ between adjacent

(70) Pauling, L. *Z. Kristallogr.* **1929**, *69*, 187.
(71) Hoekstra, H. R. *Inorg. Chem.* **1966**, *5*, 754−757.
(72) Greis, O. *J. Solid State Chem.* **1980**, *34*, 39−44.
(73) Zhou, W.; Jefferson, D. A.; Liang, W. Y. *Surf. Sci.* **1989**, *1989*, 444−454.
(74) Le Van, T.; Che, M.; Kermarec, M.; Louis, C.; Tatibouët, J. M. *Catal. Lett.* **1990**, *6*, 395−400.
(75) Squire, G. D.; Luc, H.; Puxley, D. C. *Appl. Catal. A* **1994**, *108*, 261−278.
(76) Hussien, G. A. M.; Gates, B. C. *J. Chem. Soc., Faraday Trans.* **1996**, *92*, 2425−2430.
(77) Palmer, M. S.; Neurock, M.; Olken, M. *J. Phys. Chem. B* **2002**, *106*, 6543−6547.

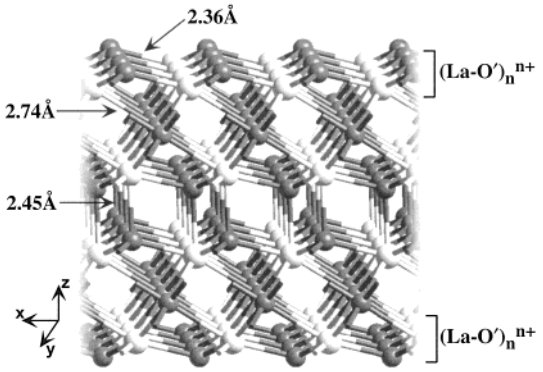


***Figure 3.*** Symmetric, stoichiometric $La_2O_3(001)$ slab. Both faces of the slab expose $(La-O')_n^{n+}$ double-hexagonal layers. The bond lengths shown are for the optimized slab at the equilibrium lattice constants, $a = b =$ 3.95 Å.

$(LaO')_n^{n+}$ layers to expose O′ and six-coordinate La atoms on both faces (Figure 3). Since the stoichiometry of the unit cell is maintained, all of the oxygen ions, including those on the surface, can be viewed formally as $O^{2-}$ anions. Geometry optimization of the stoichiometric $La_2O_3(001)$ slab does not lead to any significant structural changes as compared to the optimized bulk structure. Adsorption of hydrogen at a surface $O^{2-}$ site, however, results in the H-bound oxygen ion "lifting" off the surface, as evidenced by the La−O′ bond lengths increasing from 2.36 to 2.62 Å. The O′−H bond distance optimizes to 0.98 Å.

The adsorption energy of hydrogen at an $O^{2-}$ surface site was calculated to be −19.7 kcal/mol. Both Au et al.[45] and Yu and Anderson[78] have suggested that the weak O−H binding associated with surface oxide sites stems from the closed-shell nature of the oxide system. Au et al. based this conclusion on results of cluster calculations specifically designed to model an $O^{2-}$ site. They found that the highest occupied molecular orbital (HOMO) of the seven-atom cluster $[La_3O_4]^+$ is predominantly oxygen in character and completely filled. In a localized picture, the HOMO of $[La_3O_4]^+$ can be viewed as an $sp^3$-hybridized orbital centered on the "surface" oxygen containing a lone-pair of electrons. Interaction between the high-energy, lone-pair electrons and one of the C−H $\sigma$ bonding orbitals of methane leads to a destabilizing, two-orbital/four-electron interaction. Likewise, interaction between $O^{2-}$ and the lone electron of an isolated hydrogen atom is also unfavorable. Although methane/hydrogen is capable of binding to higher energy, unoccupied, antibonding oxygen-based orbitals, the result is a weak O−H adsorption energy. An analogous line of reasoning can be applied to the $La_2O_3(001)$ slab. Since lanthanum oxide is an insulating material, the bands are fully filled through the Fermi level, and there exists a sizable band gap (the calculated band gap is 3.81 eV, and literature values range between 2.8 and 5.4 eV).[79,80] Partial density of states (DOS) plots (Figure 4) reveal that bands near the Fermi level have a sizable contribution from the surface oxygen atoms, and Pauli repulsion between electrons in these bands and the electrons of the adsorbates dominates. As a result, the only stabilizing interaction between $CH_4$/H and the surface involves higher energy bands, which leads to a weakly bound, physisorbed species.

(78) Yu, J. W.; Anderson, A. B. *J. Am. Chem. Soc.* **1990**, *112*, 7218−7221.
(79) Estell, T. H.; Flenges, S. N. *J. Electrochem. Soc.* **1969**, *116*, 771−778.
(80) Derbeneva, S. S.; Batsanov, S. S. *Dokl. Akad. Nauk SSSR* **1967**, *175*, 1062−1063.

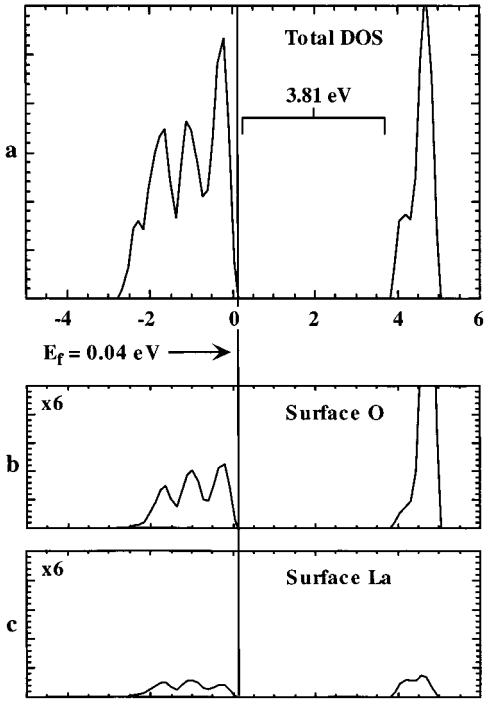


***Figure 4.*** Density of states (DOS) plots for the symmetric, stoichiometric $La_2O_3(001)$ slab: (a) the total DOS; (b) the partial DOS for the surface oxygen atoms; and (c) the partial DOS for the surface La atoms.

The overall reaction energy for a surface $(O')^{2-}$ site and methane to generate an O′−H surface species and gas-phase $^{\bullet}CH_3$ radical (eq 4) is calculated to be endothermic by 91.2 kcal/

$$(O')_{(s)}^{2-} + CH_4 \rightarrow (O')_{(s)}^{2-}-H + {}^{\bullet}CH_3 \qquad \Delta E_{rxn} = 91.6 \text{ kcal/mol} \qquad (4)$$

mol. Au and co-workers found the overall energy for the analogous reaction over the $[La_3O_4]^+$ cluster (eq 5) to be

$$[La_2O_3]^+ + CH_4 \rightarrow [La_3O_4]^+-H + {}^{\bullet}CH_3 \qquad (5)$$

endothermic by 65.3 kcal/mol.[45] Although some difference in the calculated energies between the two studies is expected due to dissimilarities in methods and structural models, it is not exactly clear why there is such a large discrepancy in overall reaction energy. The calculations we performed on the $[La_3O_4]^+$ cluster produced a hydrogen binding energy of −18.6 kcal/mol and an overall reaction energy of 93.4 kcal/mol; both energies are directly comparable to those we obtained using periodic DFT. It is worth noting that we found the energies of the adsorbate/cluster complex to be quite sensitive to structural relaxation. The fact that Au et al. did not allow for structural relaxation of the clusters may account for the difference in the calculated reaction energies.

Since the overall energy for the reaction shown in eq 4 is rather endothermic and thus unlikely to occur, we did not calculate the activation barrier for H-abstraction by an $O^{2-}$ site.

**Hydrogen Abstraction over Surface $O^-$ Sites.** Anionic $O^-$ surface sites on $La_2O_3$ were modeled by constructing an asymmetric slab from the {001} surface consisting of three lanthanum layers and five oxygen layers (Figure 5). The asymmetry of the slab results in a stoichiometric excess of oxygen (i.e., $La_2O_{3.33}$) and a formal one-electron oxidation of

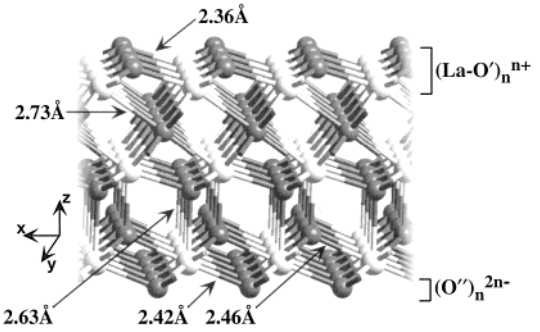


***Figure 5.*** Asymmetric, nonstoichiometric $La_2O_{3.33}$(001) slab. The upper face of the slab exposes an $(La-O')_n^{n+}$ double-hexagonal layer, and the bottom face exposes an $(O'')_n^{2n-}$ hexagonal layer. The bond lengths shown are for the optimized slab at the equilibrium lattice constants, $a = b =$ 3.95 Å.

the slab; that is, four of the oxygen layers can be described as containing $O^{2-}$ oxide ions, while the fifth oxygen layer (the surface layer) can be described formally as containing $O^-$ anions. In addition, the asymmetry leads to exposure of two different surfaces, an O′/six-coordinate La surface layer on one face of the slab and an O″/seven-coordinate La surface layer on the other face. Constructing the $La_2O_3$(001) surface in this manner results in coordinatively unsaturated oxygen atoms on both faces, but only one La−O bond per lanthanum atom was cleaved to expose the O′ layer, while three La−O bonds were cleaved to form the O″ layer. Consequently, the O′ face should be more stable and predominate under OCM condition. Indeed, different hydrogen adsorption energies and reaction energies are calculated for the two surfaces, and our results reflect the greater stability/lower reactivity of the O′-covered surface. Since it has been suggested that H-abstraction reactions occur at coordinatively unsaturated surface oxygen sites, we report our finding for both $O^-$ surfaces.

Optimization of the asymmetric $La_2O_{3.33}$(001) slab has varying effects on the two different oxygen-covered surfaces; little ionic motion is observed for the atoms near the O′-covered surface, while significant reconstruction is observed for those near the O″-covered surface. Atomic reconstruction of the O″-covered surface is two-fold: (1) the O″ atoms at the surface move inward toward the bulk, and (2) the seven-coordinate lanthanum atoms near the surface move out and away from the bulk. Both movements stem directly from the high degree of unsaturation of the O″ atoms' coordination sphere caused by cleavage of the surface. That is, the O″ atoms move toward the bulk to compensate for negative charge lost when the three La−O bonds are cleaved, and the lanthanum atoms move away from the bulk to relieve the accumulation of negative charge caused by the approaching O″ atoms. The primary result is contraction of the La−O″ bond distance from 2.74 to 2.42 Å, leaving what used to be an O″ bulk site structurally similar to a typical O′ surface site.

Adsorption of hydrogen at an oxygen site on the O′-exposed surface leads to the H-bound oxygen atom "lifting" off the surface and the associated La−O′ bond distances expanding from 2.36 to 2.60 Å. The O′−H distance optimizes to 0.97 Å. Both the La−O′ and the O′−H bond lengths are less than those calculated when hydrogen adsorbs at an $O^{2-}$ site, indicating a stronger interaction between hydrogen and the "$O^-$" site. The stronger interaction is clearly reflected in the highly exothermic hydrogen adsorption energy, which is calculated to be −102.6

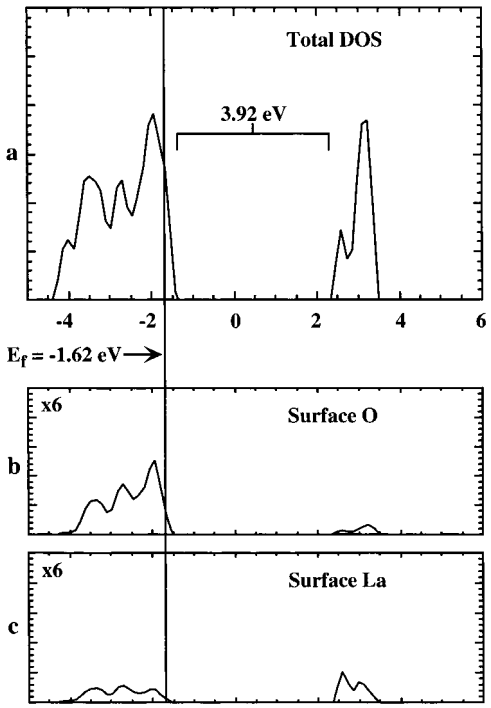


***Figure 6.*** Density of states (DOS) plots for the asymmetric, nonstoichiometric $La_2O_{3.33}$(001) slab: (a) the total DOS; (b) the partial DOS for the surface oxygen atoms; and (c) the partial DOS for the surface La atoms.

kcal/mol. This is approximately 80 kcal/mol more exothermic than hydrogen adsorption at an $O^{2-}$ site. Though the difference is marked, it is easily explained in terms of the formal oxidation of the surface brought about by the nonstoichiometry of the $La_2O_{3.33}$(001) slab. As mentioned in the discussion of the $O^{2-}$ site, partial DOS plots of a fully oxided slab show that bands near the Fermi level have a sizable contribution from the surface oxygen atoms. Oxidation of the surface removes electron density from these atoms. This is clearly evident from inspection of the total and partial DOS plots for the $La_2O_{3.33}$(001) slab (Figure 6). Consequently, hydrogen is able to interact with the incompletely filled surface-oxygen-based bands rather than interacting with higher energy bands which lie well above the Fermi energy. The result is chemisorption of the hydrogen atom rather than simple physisorption. The large hydrogen adsorption energy manifests itself in the calculated energy for the overall reaction between the surface and methane (eq 6), which was found to

$$(O')^-_{(s)} + CH_4 \rightarrow (O')^-_{(s)}-H + {}^{\bullet}CH_3 \qquad \Delta E_{rxn} = 8.2 \text{ kcal/mol} \qquad (6)$$

be only +8.2 kcal/mol. The activation energy for the H-abstraction step was calculated to be 10.1 kcal/mol. The estimated transition state structure for methane activation is shown in Figure 7. At the transition state, the C−H bond of methane which is breaking is 1.33 Å, and the O−H bond which is forming on the surface is 1.26 Å. The surface oxygen atom interacting with methane raises up out of the plane of the surface by 0.26 Å, resulting in a La−O′ distance of 2.51 Å.

Au and co-workers modeled an $O^-$ site with the $[La_3O_4]^{2+}$ cluster. They found the overall reaction energy for H-abstraction from methane (eq 7) to be −11.2 kcal/mol, with an activation

$$[La_2O_3]^{2+} + CH_4 \rightarrow [La_3O_4]^{2+}-H + {}^{\bullet}CH_3 \qquad (7)$$

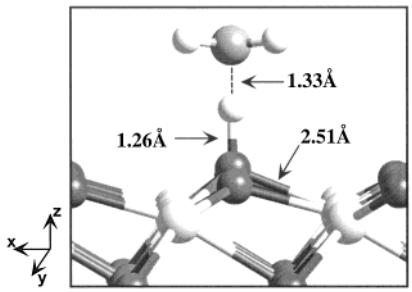


***Figure 7.*** Estimated transition-state structure for the abstraction of hydrogen from methane over an $O^-$ site of $La_2O_3(001)$.

energy of 15.0 kcal/mol.[45] We performed similar calculations on the $[La_3O_4]^{2+}$ cluster and found $\Delta E_{rxn} = -5.1$ kcal/mol and $\Delta E_{act} = 4.9$ kcal/mol. The binding energy of hydrogen was determined to be $-117.1$ kcal/mol. Both sets of calculations are certainly consistent with and in the range of the results obtained with VASP, suggesting that the same surface site is being modeled. In addition, comparison of atomic charges of the clusters shows that the "surface" oxygen atom becomes distinctly more positive on going from $[La_3O_4]^+$ to $[La_3O_4]^{2+}$, indicating that it is the surface oxygen atom which is predominantly oxidized. To further confirm the exact nature of the oxygen site, we performed a series of calculations with VASP in which the symmetric, stoichiometric $La_2O_3(001)$ slab was oxidized by removing one electron from the surface cell. Both binding energies and overall reaction energies of the oxidized slab are consistent (differences <2 kcal/mol) with the results for the O′-covered surface of the $La_2O_{3.33}(001)$ slab, again indicating the presence of a surface $O^-$ site.

The energetics of an $O^-$ site on the O″-exposed surface are similar to those of the O′-exposed surface. The binding energy for hydrogen was found to be $-118.5$ kcal/mol, whereas the overall energy of reaction and activation energy were $-7.6$ and 8.6 kcal/mol, respectively. As alluded to above, the greater exothermicity stems from the fact that the O″-exposed face of $La_2O_{3.33}(001)$ slab is a high-energy surface, which is stabilized to a greater extent by interactions with adsorbates. Though accessible O″ sites are probably not common under our reaction conditions, they could exist at step-edges or other defect sites which are known to exist on $La_2O_3$ at these reaction conditions[81,82] and may contribute to the overall OCM reactivity on $La_2O_3$.

**Formation of Active Oxygen Sites.** In addition to the fact that no $O^-$ surface species has been detected on rare-earth-metal OCM catalysts, no clear understanding of the mechanism to generate such a species exists. In an attempt to identify possible structural features which may control the formation of active $O^-$-like sites, we examined the effects of doping $La_2O_3$ with $Sr^{2+}$, creating anion vacancies in the lattice, and introducing molecular oxygen precursors. The results of each of these studies are discussed below.

**Strontium Doping.** It is well established that doping the basic $La_2O_3$ catalyst with strontium greatly enhances the activity of the material. In $Sr^{2+}$-promoted systems, conversion of methane and selectivity for $C_2$ products have been shown to increase by as much as 5% and 15%, respectively.[3,5,8] Although a number of experimental studies have been reported on the $Sr/La_2O_3$ system,[83−88] few explanations for the promotion effect have been proposed. It has been suggested, however, that $Sr^{2+}$ exchange with the $La^{3+}$ cations at the surface may give rise to localized $O^-$-like sites. Our calculations on $Sr^{2+}$-promoted systems suggest that the surface oxygen site that is formed from direct $Sr^{2+}/La^{3+}$ exchange indeed mimics an $O^-$ site. The binding energy of hydrogen at this oxygen site was calculated to be $-109.7$ kcal/mol, which is consistent with the value of $-102.6$ kcal/mol for the explicit $O^-$ site.

**Surface Oxygen Vacancies.** Surface oxygen vacancies on $La_2O_3$ were studied by removing an oxygen atom from the surface of the symmetric, stoichiometric $La_20_3(001)$ slab (see Figure 3). The defect can be viewed formally as an F-center (an oxygen hole containing two electrons). Optimization of the slab results in a slight contraction of the La−O′ bond adjacent to the F-center from 2.36 to 2.34 Å. No other reconstruction of the surface is observed. This suggests that the F-center electrons remain localized in the defect site, possibly stabilized due to the fact that they reside in a three-fold site of $La^{3+}$ cations.

When hydrogen is adsorbed on a surface oxygen atom adjacent to an F-center, its adsorption energy is calculated to be exothermic by $-26.2$ kcal/mol. The value is slightly more exothermic than the case when hydrogen adsorbs on a "pure" $O^{2-}$ surface site ($-19.7$ kcal/mol), but the difference is small, indicating that the surface oxygen atoms neighboring the F-center remain essentially $O^{2-}$-like, despite the perturbation to the surface structure. Again, this implies that the two F-center electrons remain primarily localized in the defect. Further evidence that the electrons remain localized is reflected in the fact that adsorption of hydrogen at an oxygen site adjacent to the hole results in the H-bound oxygen ion "lifting" off the surface by a similar amount as the case when no defect exists; i.e., the bond length between the H-bound oxygen atom and the surrounding surface La atoms is 2.60 Å when an F-center is adjacent to the adsorption site and 2.62 Å when no defect is near the adsorption site. Likewise, the O′−H bond distance is 0.98 Å both with and without a neighboring F-center.

**Molecular Oxygen Precursors.** We found that molecular oxygen is capable of binding at an F-center with an adsorption energy of $-154.6$ kcal/mol. The orientation of the $O_2$ moiety bound in the hole is such that it lies at an angle of 27.3° with respect to the plane of the surface (Figure 8). The oxygen atom nearest the surface is shifted slightly from the three-fold La site typical of surface oxide ions and closer to a La-atop site, allowing the upper oxygen atom to align itself directly above a La−La bridge site. This "bent" orientation is advantageous over one in which $O_2$ adsorbs at the F-center perpendicular to the surface ($\Delta E_{ads} = -150.4$ kcal/mol), since it allows the three $La^{3+}$ cations around the hole site to stabilize the negative charge on *both* oxygen atoms of the $O_2$ moiety rather than only one. Adsorption of $O_2$ expands the O−O distance from 1.24 to 1.47

(81) Lacombe, S.; Geantet, C.; Mirodatos, C. *J. Catal.* **1994**, *151*, 439−452.
(82) Mirodatos, C.; Xu, G.; Lacombe, S.; Ducarme, W.; Martin, G. A. Structure Sensitivity of Oxidative Coupling of Methane and Dehydrogenation of Ethane Over Lanthana Catalysts. In *Natural Gas Conversion IV*; de Pontes, M., Espinoza, R. L., Nicolaides, C. P., Scholz, J. H., Scurrell, M. S., Eds.; Studies in Surface Science and Catalysis 107; Elsevier Science B.V.: New York, 1997; pp 345−350.
(83) DeBoy, J. M.; Hicks, R. F. *J. Catal.* **1988**, *113*, 517−524.
(84) Gulcicek, E. E.; Colson, S. D.; Pfefferle, L. D. *J. Phys. Chem.* **1990**, *94*, 7069−7074.
(85) Kalenik, E.; Wolf, E. E. *Catal. Lett.* **1991**, *9*, 441.
(86) Feng, Y.; Niiranen, J.; Gutman, D. *J. Phys. Chem.* **1991**, *95*, 6558−6563.
(87) Feng, Y.; Niiranen, J.; Gutman, D. *J. Phys. Chem.* **1991**, *95*, 6564−6568.
(88) Xu, M.; Lunsford, J. H. *Catal. Latt.* **1991**, *11*, 295−300.

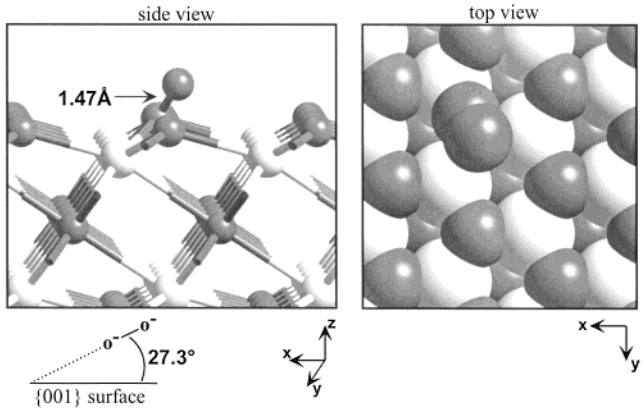


***Figure 8.*** Calculated structure of a surface peroxide site on $La_2O_3(001)$.

Å. The calculated bond length is characteristic of classical peroxides ($1.49 \pm 0.02$ Å).[89,90]

Although calculational evidence of a surface peroxidic species on $La_2O_3$ is encouraging, its formation, in the current context, depends on the existence of an F-center. Huang and co-workers[12] have suggested that pairs of F-centers could possibly be generated by desorption of molecular oxygen from the surface (eq 8). We calculate the overall reaction energy for this process

$$2O^{2-}_{(s)} \rightleftharpoons 2[\square/2e^-) + O_{2(g)},$$
$$\text{where } (\square/2e^-) \text{ represents an F-center} \qquad (8)$$

to be 312.3 kcal/mol. The highly endothermic energy is congruent with the strong binding energy of the surface oxygen atoms (−224.5 kcal/mol) and indicates that desorption of $O_2$ from the surface is unfavorable. This finding is also consistent with the limited amount of experimental evidence for F-centers on $La_2O_3$.

While F-centers may exist due to impurities and structural defects or be formed by means more energetically favorable than desorption of molecular oxygen, we were curious whether a similar peroxide-like species could be generated without requiring the presence of an F-center. We found that it is possible to dissociatively adsorb molecular oxygen on an oxide-($O^{2-}$)-covered surface (Figure 9).[77] Surprisingly, the overall reaction energy for this process (eq 9) is calculated to be only

$$2O^{2-}_{(s)} + O_{2(g)} \rightarrow 2O^{2-}_{2(s)}$$
$$\Delta E_{rxn} = 12.1 \text{ kcal/mol} \qquad (9)$$

12.1 kcal/mol, with an apparent activation energy of 33.0 kcal/mol. The surface peroxides formed by dissociative adsorption of $O_2$ are essentially identical to those formed by chemisorption of $O_2$ at F-centers. The $O_2^{2-}$ moieties are bent with respect to the surface at an angle of approximately 25°, and the new O′−O bonds are 1.47 Å. The original O−O bond of the gas-phase $O_2$ is lengthened to 2.67 Å and essentially broken.

The only other description of a peroxide-like species on OCM catalysts is that of a "nonclassical" peroxide. Nonclassical peroxides have been characterized as a through-bond species involving two isolated yet coupled $O^-$ surface anions. Simulations by Islam and Illet[50,51] on $La_2O_3(011)$ predicted an $O^-$−$O^-$ distance of 3.9 Å, and experiments by Lunsford and Kharas[20] on $BaPbO_3$ indicated an $O^-$−$O^-$ contact of ∼3.0 Å. Lunsford and Kharas noted, however, that crystallographic analysis of $BaPbO_3$ was based on a profile refinement of powder data which included high *R*-factors. Regardless of the validity of these claims, it is clear from our results that it is not necessary to describe surface peroxide species on $La_2O_3$ in a nonclassical manner. Classical $O_2^{2-}$ surface species can be formed either by adsorption of molecular oxygen at F-centers or, more likely, by dissociative adsorption of $O_2$ directly on the oxide surface.

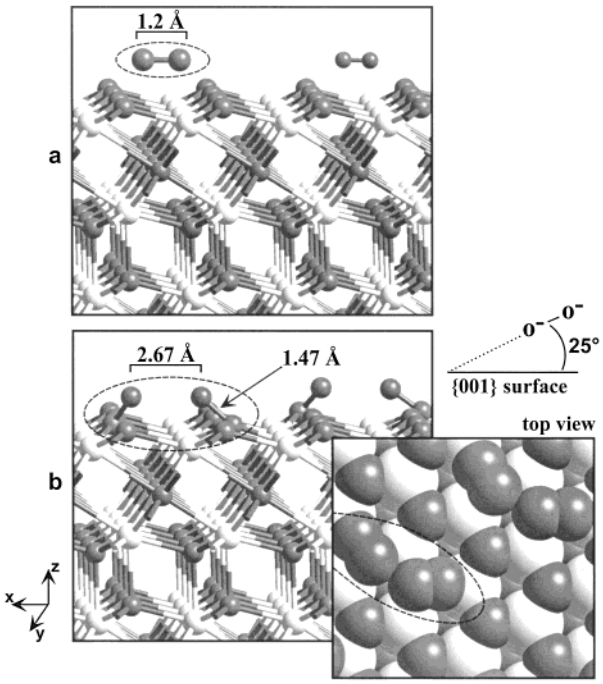


***Figure 9.*** Calculated structure of surface peroxide sites on $La_2O_3(001)$ formed by dissociative adsorption of molecular $O_2$: (a) the reactant state and (b) the product state.

**Hydrogen Abstraction over Surface $O_2^{2-}$ Sites.** Surface peroxides on $La_2O_3$ offer two potential oxygen sites at which H-abstraction reactions can occur: a lower, embedded $O^-$ site and an upper, exposed $O^-$ site (see *side view* of Figure 8). Hydrogen binds to the upper, exposed oxygen atom of the surface $O_2^{2-}$ species with an adsorption energy of −71.5 kcal/mol. This is approximately 52 kcal/mol more exothermic than an $O^{2-}$ site and 31 kcal/mol less exothermic than an $O^-$ site. Adsorption leads to elongation of the peroxide O′−O bond from 1.47 to 2.19 Å. In addition, the bonds between the surface La atoms and the lower oxygen atom of the $O_2^{2-}$ moiety contract to values typical of an oxide-covered surface (2.37 Å). Taken together, the structural data indicate that the interaction between the surface and the O−H species is weak and may be easily cleaved to regenerate the catalytic surface. The $\Delta E_{rxn}$ for the exposed peroxide site and methane to generate an O−H surface species and gas-phase $^{\bullet}CH_3$ radical (eq 10) is calculated to be

$$O^{2-}_{2(s)} + CH_4 \rightarrow O^{2-}_{2(s)}\text{−H} + {}^{\bullet}CH_3$$
$$\Delta E_{rxn} = 39.3 \text{ kcal/mol} \qquad (10)$$

39.3 kcal/mol. The overall reaction energy for this process is 31 kcal/mol more endothermic than that for H-abstraction over an $O^-$ site. The activation energy is 47.3 kcal/mol. The structural features at the transition state are similar to those of the $O^-$ site; i.e., the C−H bond which is breaking is 1.31 Å and the

(89) Vannerberg, N.-G. *Prog. Inorg. Chem.* **1962**, *4*, 125−197.
(90) Boca, R. *Coord. Chem. Rev.* **1983**, *50*, 1−72.

O−H bond which is forming is 1.20 Å. Even though the activation energy is relatively high, H-abstraction over the peroxide site remains energetically accessible because of the 600−700 °C temperatures typically employed during OCM.

Hydrogen does bind to the lower, embedded oxygen atom of the surface peroxide, but $\Delta E_{ads}$(H) is approximately 10 kcal/mol less exothermic than at the upper oxygen site. The decreased activity most likely stems from stabilization of the negative charge on the embedded oxygen atom by the surface $La^{3+}$ cations. The negative charge on the exposed oxygen atom of the peroxide is not stabilized to any extent by the surface ions and is thus more active for hydrogen abstraction.

Attempts to model hydrogen binding simultaneously at both oxygen atoms of a surface peroxide species were unsuccessful. This suggests that generation of carbene radicals directly from methane at a single, isolated surface peroxide site, as suggested by Au et al. to account for ethylene production over $BaCO_3$/LaOBr catalysts,[25] may not be likely or at least not universal over REM oxide catalysts. A viable alternative, however, is simultaneous abstraction of two H atoms from methane at neighboring peroxide sites to generate methylene radicals which could then couple in the gas phase to form ethylene directly. Abstraction of two hydrogen atoms directly from ethane at peroxide pairs could also result in ethylene formation. Each of these pathways will be explored in a future publication.

**General Comments on the Mechanism of OCM over $La_2O_3$: Active Site Formation, C−H Bond Activation, and Catalyst Regeneration.** Our results indicate that anionic $O^-$ sites should be the most active species on $La_2O_3$. While no $O^-$ species has yet been identified on a REM oxide, the possible role of such a species in OCM chemistry cannot be rejected. We found that doping strontium into the $La_2O_3$ surface via $Sr^{2+}$/$La^{3+}$ exchange generates a surface oxygen site characteristic of an $O^-$ species, which may account for the enhanced OCM reactivity of Sr-doped $La_2O_3$ catalysts when compared to the unpromoted system. This finding is supported by methane activation energies reported by Lunsford et al.; they reported that activation energies for methyl radical production from methane over $Sr/La_2O_3$[88] and Li/MgO,[91] a catalyst widely believed to operate via surface $O^-$ sites, are both approximately 23 kcal/mol. In contrast, Otsuka and Jinno determined an activation energy of 37 kcal/mol for the production of $^{\bullet}CH_3$ from methane over $Sm_2O_3$,[16] and Lunsford et al. reported a barrier of 63 kcal/mol over $Mn/Na_2WO_4/SiO_2$.[15] In these systems, a slightly less active oxygen intermediate may be important in H-abstraction chemistry. Experiment and theory both indicate that a surface peroxide species is a likely candidate. Experimental studies have not only identified surface peroxides on a number of REM catalysts but also, in some instances, have provided evidence for the active role of $O_2^{2-}$ species in OCM chemistry, and our theoretical results show that $O^-_{(s)}$ and $O_2^{2-}{}_{(s)}$ are not that dissimilar with respect to the energetics of H-abstraction from $CH_4$. Consequently, we focus our discussion of the mechanism of OCM over $La_2O_3$(001) to catalytic pathways involving surface peroxides as the active surface oxygen species.

Lunsford and co-workers have provided a number of clues regarding the overall mechanism of OCM over $La_2O_3$ from a series of studies concerning the formation of hydroxyl radical during the reaction of oxygen with methane or water over basic lanthanide oxide catalysts.[92−94] Using laser-induced fluorescence spectroscopy, the Lunsford group has shown that strongly basic oxides are capable of generating $^{\bullet}OH$ radicals at the catalyst surface; the radicals then emanate into the gas phase. Reaction of molecular oxygen and methane over $La_2O_3$ generates gas-phase $^{\bullet}OH$ radicals and $H_2O$. When $CH_4$ is replaced with an equivalent amount of $H_2O$, the concentration of $^{\bullet}OH$ radicals increases. Competition studies show that addition of $CH_4$ to the $O_2/H_2O$ system has a strong, negative effect on the production of $^{\bullet}OH$ radicals, indicating that the same type of active surface center is responsible for formation of $^{\bullet}CH_3$ radicals from $CH_4$ and $^{\bullet}OH$ radicals from $H_2O$. Lunsford and co-workers also found that production of $^{\bullet}CH_3$ radicals is kinetically limited, whereas the production of $^{\bullet}OH$ radicals is limited only by thermodynamics. This is reflected in the fact that the $^{\bullet}OH$ radical concentration in the $O_2/CH_4$ system is directly related to the amount of $H_2O$ produced at the catalyst surface, while the concentration of $^{\bullet}OH$ in the $O_2/H_2O$ system is controlled through an equilibrium with the reagents. In other words, all of the $^{\bullet}OH$ radicals produced in the reaction of the $O_2/CH_4$ or $O_2/H_2O$ systems appear to be formed via H-abstraction from $H_2O$.

Keeping these experimental observations in mind, we find that the reaction of oxygen with methane over an oxide-covered surface of $La_2O_3$(001) to form a $^{\bullet}CH_3$ radical at a surface peroxide site (eq 11) is endothermic by 40.8 kcal/mol. Reaction

$$O^{2-}_{(s)} + {}^1/_2O^2 + CH_4 \rightarrow O^{2-}_{2(s)}-H + {}^{\bullet}CH_3 \qquad \Delta E_{rxn} = 40.8 \text{ kcal/mol} \tag{11}$$

of oxygen with $H_2O$ to form an $^{\bullet}OH$ radical at a surface peroxide site (eq 12) is endothermic by 50.9 kcal/mol. Assuming that

$$O^{2-}_{(s)} + {}^1/_2O_2 + H_2O \rightarrow O^{2-}_{2(s)}-H + {}^{\bullet}OH \qquad \Delta E_{rxn} = 59.0 \text{ kcal/mol} \tag{12}$$

similar active sites are indeed involved in H-abstraction from both $CH_4$ and $H_2O$, it is clear from a comparison of $\Delta E_{rxn}$ values for the reactions shown in eqs 11 and 12 that abstraction from $CH_4$ is energetically favored. This agrees with Lunsford's experiments, showing that addition of $CH_4$ to the $O_2/H_2O$ system has a strong, negative effect on the production of $^{\bullet}OH$ radical.

Two potential routes exist for generating $^{\bullet}OH$ radicals in the $O_2/CH_4$ system once H-abstraction over the surface peroxide site has occurred (eq 13).

$$O^{2-}_{2(s)}-H \rightarrow O^{2-}{}_{(s)} + {}^{\bullet}OH \qquad \Delta E_{rxn} = 34.3 \text{ kcal/mol} \tag{13a}$$

$$O^{2-}_{2(s)}-H \rightarrow {}^1/_2O^{2-}_{(s)} + {}^1/_2O^{2-}_{2(s)} + {}^1/_2H_2O \qquad \Delta E_{rxn} = -11.5 \text{ kcal/mol} \tag{13b}$$

The first route involves simple dissociation of $^{\bullet}OH$ radical from the surface, leaving behind an oxide $O^{2-}{}_{(s)}$ site (eq 13a). The overall reaction energy for this process is highly endothermic

(91) Xu, M.; Shi, C.; Yang, X.; Rosynek, M. P.; Lunsford, J. H. *J. Phys. Chem.* **1992**, *96*, 6395−6398.

(92) Anderson, L. C.; Xu, M.; Mooney, C. E.; Rosynek, M. P.; Lunsford, J. H. *J. Am. Chem. Soc.* **1993**, *115*, 6322−6326.

(93) Hewett, K.; Anderson, L. C.; Rosynek, M. P.; Lunsford, J. H. *J. Am. Chem. Soc.* **1996**, *118*, 6992−6997.

(94) Hewett, K.; Rosynek, M. P.; Lunsford, J. H. *Catal. Lett.* **1997**, *45*, 125−128.

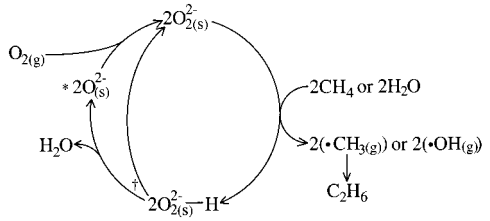


***Figure 10.*** Proposed mechanism for OCM over $La_2O_3(001)$ involving surface peroxide sites; ∗ indicates start of catalytic cycle; † indicates that one $O^{2-}{}_{(s)}$ and one $O_2{}^{2-}{}_{(s)}$ site are regenerated via elimination of $H_2O$ from the surface.

(57.4 kcal/mol), suggesting that formation of $^\bullet$OH radical directly from a surface intermediate is unlikely. This route is also inconsistent with Lunsford's findings. Alternatively, the surface O−H species can be eliminated as $H_2O$, leaving behind 1 equiv each of $O^{2-}_{(s)}$ and $O^{2-}_{2(s)}$ surface sites (eq 13b). Although eq 13b shows the reaction as a single elementary step, elimination of $H_2O$ likely involves reaction of one surface O−H group with a hydrogen atom from a neighboring O−H surface species. The $\Delta E_{rxn}$ for the overall process is −11.5 kcal/mol. The exothermic reaction energy for this particular route, the formation of $H_2O$, and the intrinsic kinetic dependence of $^\bullet$OH radical formation on the production of $H_2O$ at the surface are all consistent with Lunsford's experimental data.

With the support of experimental observations and the results of our calculations, it is possible to suggest a plausible mechanism for the oxidative coupling of methane over $La_2O_3$. The ideas are incorporated into the catalytic cycle shown in Figure 10. The cycle is initiated by dissociative adsorption of molecular oxygen over an oxide-covered surface to form a pair of surface peroxide sites. Hydrogen abstraction from both $CH_4$ and $H_2O$ occurs at the surface $O_2{}^{2-}$ sites, though abstraction from methane is energetically favored. Abstraction from $CH_4$ generates a gas-phase $^\bullet CH_3$ radical, whereas abstraction from $H_2O$ generates a gas-phase $^\bullet$OH radical. The $^\bullet CH_3$ radicals couple in the gas phase to form $C_2H_6$. Catalyst regeneration occurs by elimination of $H_2O$ and concomitant reformation of $O^{2-}_{(s)}$ and $O^{2-}_{2(s)}$ sites.

## Summary

A summary of our results for H-abstraction from methane at $O^{2-}_{(s)}$, $O^{-}_{(s)}$, and $O^{2-}_{2(s)}$ sites on $La_2O_3(001)$ is shown in Table 1. The most active surface oxygen site was found to be the anionic $O^-$ species. The overall reaction energy for the activated surface and methane to generate an O−H surface species and gas-phase $^\bullet CH_3$ radical (eq 6) was found to be nearly thermoneutral and to have an activation barrier of 10.1 kcal/mol. The adsorption energy of hydrogen at this site was calculated to be in excess of −100 kcal/mol. We found that a similar oxygen site could be generated by a one-for-one $La^{3+}/Sr^{2+}$ exchange at the surface. Though anionic $O^-$ species have not been identified on REM oxide catalysts under OCM conditions, this may account for the enhanced activity of the Sr-doped $La_2O_3$ system.

***Table 1.*** Comparison of H-Adsorption Energies, Overall Reaction Energies,[a] and Activation Energies (in kcal/mol) for H-Abstraction from Methane at Various $La_2O_3$ Surface Oxygen Sites

| | $\Delta E_{ads}$(H) | $\Delta E_{rxn}$($CH_4$) | $\Delta E_{act}$(H-abstraction) |
|---|---|---|---|
| $O^{2-}$ | −19.7 | 91.6 | |
| $(O^{2-})^b$ | −26.2 | 84.7 | |
| $O^-$ (O′) | −102.6 | 8.2 | 10.1 |
| $O^-$ (O″) | −118.5 | −7.6 | 8.6 |
| $(O^-)^c$ | −109.7 | 1.2 | |
| $O_2{}^{2-}$ | −71.5 | 39.3 | 47.3 |

[a] Overall reaction energy for a surface oxygen species and methane to generate an O−H surface species and gas-phase $^\bullet CH_3$ radical ($O_n{}^{m-} + CH_4 \rightarrow O_n{}^{m-}-H + {}^\bullet CH_3$). [b] Surface $O^{2-}$ site adjacent to an F-center. [c] Created by $Sr^{2+}/La^{3+}$ exchange at the $La_2O_3(001)$ surface.

While oxygen point defects did not enhance reactivity at neighboring surface oxygen sites, we found that surface peroxides can be generated by adsorption of molecular oxygen at defect sites, as well as by dissociative adsorption of molecular oxygen across the closed-shell oxide surface of $La_2O_3(001)$. The overall reaction energy for the latter pathway is calculated to be only 12.1 kcal/mol, with an apparent activation energy of 33.0 kcal/mol. This finding is in agreement with experimental isotopic labeling studies which suggest that dissociative adsorption of $O_2$ occurs readily over OCM catalysts. Irrespective of the route to peroxide formation, the $O^{2-}_{2(s)}$ intermediate is characterized by a bent orientation with respect to the surface and an O−O bond length of 1.47 Å. Both attributes are consistent with structural features characteristic of classical peroxides. We found surface peroxide sites to be slightly less favorable for H-abstraction from methane than the $O^{-}_{(s)}$ species, with $\Delta E_{rxn}(CH_4) = 39.3$ kcal/mol, $E_{act} = 47.3$ kcal/mol, and $\Delta E_{ads}(H) = -71.5$ kcal/mol. While the activation energy is relatively high, it remains energetically accessible because of the 600−700 °C temperatures typically employed during OCM.

On the basis of the results of our calculations and others' experimental data, it is possible to propose a mechanism for OCM over $La_2O_3(001)$ involving surface peroxides as the active oxygen source. The mechanism involves dissociative adsorption of molecular oxygen over the oxide-covered surface to form surface peroxide sites, H-abstraction from $CH_4$ at the surface $O_2{}^{2-}$ sites, coupling of gas-phase $^\bullet CH_3$ radicals to produce ethane, and catalyst regeneration by elimination of $H_2O$ and regeneration of $O^{2-}_{(s)}$ and $O^{2-}_{2(s)}$ sites.

**Acknowledgment.** We kindly acknowledge financial support from The Dow Chemical Co. We thank the Office for Information Technology and Communication (ITC) at UVa, the Computer Science Department at UVa, and NCSA at the University of Illinois at Urbana−Champaign (Grant No. CTS 000028N) for valuable computer time. We also thank Dr. Georg Kresse (Institut für MaterialPhysik, Technische Universität Wien) for the La PAW pseudopotential used in our VASP calculations.

JA0121235